

# Calculating electron transport in a tight binding model of a field-driven molecular wire: Floquet theory approach

Alexander Tikhonov and Rob D. Coalson<sup>a)</sup>

*Department of Chemistry, University of Pittsburgh, Pittsburgh, Pennsylvania 15260*

Yuri Dahnovsky

*Department of Physics and Astronomy, and Department of Chemistry, University of Wyoming, Laramie, Wyoming 82071*

(Received 4 May 2001; accepted 12 December 2001)

This paper considers electron transport through a molecular bridge coupled to two metal electrodes in the presence of a monochromatic radiation field. Current flow through the wire is calculated within a nondissipative one-electron tight binding model of the quantum dynamics. Using Floquet theory, the field-driven molecular wire is mapped to an effective time-independent quantum system characterized by a tight-binding Hamiltonian with the same essential structure as the nondriven analog. Thus, Green's Function methods for computing current flow through the wire, which have been profitably applied to the molecular wire problem in the absence of driving, can also be used to analyze the corresponding field-driven system. Illustrative numerical calculations on a simple model system are presented. © 2002 American Institute of Physics. [DOI: 10.1063/1.1448292]

## I. INTRODUCTION

Conduction of electrons through a single molecule connecting two metal electrodes has received significant attention recently.<sup>1–3</sup> Experimental studies using both scanning tunneling microscopies (STM) and mechanical break junctions have been performed.<sup>4,5</sup> The experimental configuration consisting of an STM tip in proximity to an adsorbate on a metal surface provides a good example of an electrode-molecular wire-electrode system. Current-voltage (I-V) characteristics can be recorded when the tip is positioned above the adsorbate. Extensive work toward the fabrication of conducting nanowires using nanolithography techniques is underway.<sup>1</sup> A related problem of recent interest is conductance through mesoscopic systems composed of semiconductor heterostructures.<sup>6,7</sup>

The theory of conductance through molecular wires has been extensively developed. One widely utilized approach considers the relevant electron transport as a scattering process, with the molecular bridge treated in a tight-binding approximation<sup>8–10</sup> or using density-functional theory.<sup>11</sup> In this work we apply a similar scattering theory approach to the problem of electron transport through a molecular wire in the presence of a monochromatic electromagnetic field (provided, for example, by a laser).

Theoretical analyses suggest that illumination of the molecular bridge by an intense laser field can alter the conductance properties of different molecular bridge systems, including long-range metal-metal electron transfer intramolecular complexes,<sup>12</sup> double-barrier semiconductor heterostructures,<sup>13</sup> and STM systems.<sup>14</sup> (In an STM system the gap between the surface and the tip is illuminated.) The purpose of the present report is to develop an analogous theory for the effect of radiation on electronic conduction

between two metal electrodes through a simple organic molecule (“molecular wire”).

To date, experimental evidence for ac field modified transfer of electron transfer-transport is rather scant. However, one encouraging example is provided by the studies of Gossard and co-workers.<sup>7</sup> Upon illumination of a multi-quantum well semiconductor heterostructure with an appropriate monochromatic radiation source, they were able to strongly alter the current flow through the heterostructure. In particular, they were able to reverse the direction of current flow relative to the direction dictated by a static applied bias potential. These findings provide some motivation to search for similar effects in molecular wire systems.

We outline here a simple theoretical framework for understanding electron transport through a molecular wire in the presence of a monochromatic radiation field, which we shall also refer to as a “laser field.” We adopt the simplest theoretical model possible, namely a one-electron model of the electron transfer in the absence of environmental coupling (e.g., disorder, dissipation, etc.). In this work we focus on the theoretical framework for describing the electron transport within our prototypical model. A companion paper (to be referred to as Paper II) will present an application to a realistic molecular wire system within the framework of the model developed here.<sup>15</sup>

The outline of this paper is as follows: In Sec. II we briefly review the one-electron tight binding model of electron transport through a (nondriven) molecular wire connected to two metal electrodes, ignoring, for simplicity, dissipative coupling to nonelectronic environmental degrees of freedom. We summarize the description of current flow through the wire, focusing on a well-known Green's function based formula that prescribes the magnitude of this current in terms of the properties of the bridge molecule, the metal electrodes, and the electronic coupling between them. In Sec. III, we introduce an applied time-dependent monochromatic

<sup>a)</sup>Electronic mail: rob@ringo.chem.pitt.edu

electric field (provided by a laser), and indicate how this modifies the relevant tight-binding Hamiltonian. Using Floquet theory, we then show in Sec. IV how to map the time-dependent Hamiltonian which describes the field-driven system precisely into a time independent Hamiltonian corresponding to an augmented state space. The essential structure of this Floquet Hamiltonian is identical to that of the standard (non-driven) molecular wire problem—only the details of the effective molecular wire, the reservoirs and the coupling between them change. Thus, the Green's function formula for current flow through the non-driven wire can be readily adapted to calculate current flow for the *field driven* wire. In Sec. V, we provide an approximate way to simplify the Floquet Hamiltonian associated with the field-driven system which enables the current to be analyzed in terms of a physically appealing “independent channel” picture. The conditions of validity of the independent channel approximation (ICA) are discussed. In Sec. VI, prototypical numerical illustrations are presented for a simple model of a field-driven wire. Exact numerical integration of the time-dependent Schrödinger equation is compared to Green's function analysis of the Floquet Hamiltonian—good agreement is obtained. In addition, results of the ICA are presented to illustrate the range of its accuracy. Finally, Discussion and Conclusions are provided in Sec. VII.

## II. TIGHT BINDING MODEL OF A (NONDRIVEN) MOLECULAR WIRE

In this section we review relevant features of an electron transfer system consisting of a molecule (“molecular wire”) bridging between two metal electrodes in the presence of a static applied voltage. Additional features associated with illumination of this system via monochromatic light are discussed in the next section.

A simple one-electron tight binding model of a molecular wire<sup>8,9</sup> is schematically depicted in Fig. 1. It is comprised of two reservoirs, left and right, which represent metal electrodes, and are connected by a molecular bridge (“wire”). The overall system Hamiltonian is defined by the following features. The left reservoir states are denoted as  $|i\rangle$  and have energy  $\epsilon_i$ . They are not directly coupled to each other. The same is true of the right reservoir states, which are denoted as  $|f\rangle$  and have energy  $\epsilon_f$ . Left and right reservoir states are not coupled directly to each other. The molecular electronic structure is also represented by a tight binding Hamiltonian. The  $N$  atomic orbitals are denoted  $|I\rangle$ , with site energies  $\epsilon_I$ . These states are coupled by matrix elements  $V_{I,J}$ . Finally, coupling between the L-reservoir state  $i$  and atomic orbital  $I$  on the molecular bridge is designated by  $V_{i,I}$ . Analogously,  $V_{f,I}$  designates coupling between R-reservoir state  $f$  and bridge atomic orbital  $I$ .

The site energy levels just introduced refer to the system in the absence of any external perturbations. In order to get current to flow through the wire, some external field must be applied. In the usual case, a static, field is applied across the metal electrodes using a battery.<sup>1–6,8–11</sup> This field modifies the electronic Hamiltonian, and in particular, in the one-electron picture adopted here, changes the site energies associated with the tight binding model. We shall term the static

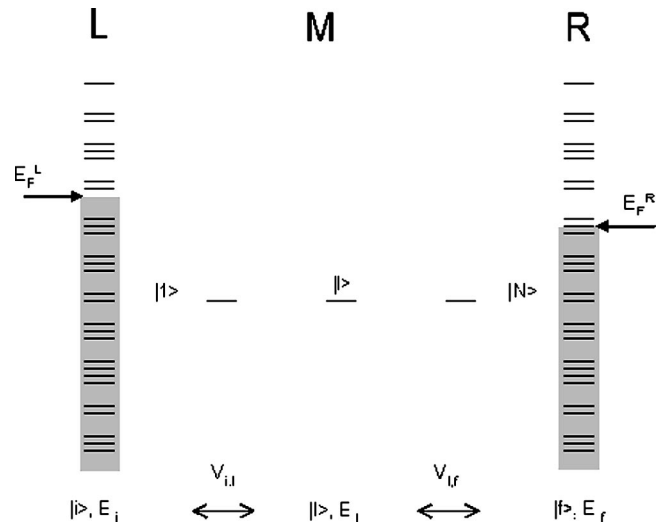


FIG. 1. Energy level and coupling diagram for a nondriven molecular wire connected to reservoirs of metallic states. Positions of left and right Fermi levels [for applied voltage  $V_{ap} = (E_F^L - E_F^R)/e_0$ ] are indicated.

field-dependent site energies as  $E_i$  for the left reservoir, etc. If the electric potential associated with the applied electric field is designated as  $\phi(\mathbf{r})$ , then

$$E_i = \epsilon_i, \quad E_I = \epsilon_I - e_0 \phi_{I,I}, \quad E_f = \epsilon_f - e_0 V_{ap}, \quad (1)$$

where  $e_0$  is the magnitude of the electronic charge, and  $\phi_{I,I} = \langle I | \phi(\mathbf{r}) | I \rangle$ . Here the electric potential  $\phi$  is taken, without loss of generality, to be zero throughout the left reservoir and have the value  $V_{ap}$  throughout the right reservoir. The precise functional form of  $\phi$  is complicated by a number of factors,<sup>9</sup> but does not affect the formal development of the one-electron model of molecular wire theory.

Bearing in mind this shift in the “bare” site energies (i.e., the molecular site energies in the absence of a static applied voltage), the Hamiltonian operator for the system when a static voltage is applied across the electrodes reads

$$\begin{aligned} \hat{H} = & \sum_i E_i |i\rangle \langle i| + \hat{H}^M + \sum_f E_f |f\rangle \langle f| \\ & + \sum_I \sum_i V_{i,I} |i\rangle \langle I| + |I\rangle \langle i| \\ & + \sum_I \sum_f V_{f,I} |f\rangle \langle I| + |I\rangle \langle f|, \end{aligned} \quad (2)$$

with the bridge Hamiltonian given by

$$\hat{H}^M = \sum_I E_I |I\rangle \langle I| + \sum_{I \neq J} V_{I,J} |I\rangle \langle J|. \quad (3)$$

Associated with the Hamiltonian  $\hat{H}$  is a state vector of the form

$$|\psi(t)\rangle = \sum_i c_i(t) |i\rangle + \sum_I c_I(t) |I\rangle + \sum_f c_f(t) |f\rangle. \quad (4)$$

Thus the time-dependent Schrödinger equation (SE),  $i|\dot{\psi}(t)\rangle = \hat{H}|\psi(t)\rangle$ , is converted into a set of first-order ordi-

nary differential equations (ODE's) of the form  $i\dot{c}_\alpha(t) = \sum_\beta H_{\alpha,\beta} c_\beta(t)$  with  $\alpha, \beta = i, I, f$ . [Note: We set  $\hbar = 1$  throughout.]

The basic dynamical scenario of interest is as follows. The system (electron) is prepared at  $t=0$  in a single state  $i_0$  of the L-reservoir. We wish to calculate the time evolution of the system for  $t > 0$ , and in particular the probability that the electron makes a transition to state  $f_0$  of the R-reservoir, i.e.,  $|c_{f_0}(t)|^2$ . From this we can compute the electrical current through the wire.

Formally,  $c_{f_0}(t) = \langle f_0 | \exp(-i\hat{H}t) | i_0 \rangle$ , and thus is related to the (retarded) Green's function<sup>16</sup> of the system via

$$\int_0^\infty dt e^{iEt - \eta t} \langle f_0 | e^{-i\hat{H}t} | i_0 \rangle = \frac{1}{i} \langle f_0 | (\hat{H} - E - i\eta)^{-1} | i_0 \rangle, \quad (5)$$

with  $\eta \rightarrow 0^+$ . The structure of the Hamiltonian enables a useful simplification of the overall Green's function, namely

$$\int_0^\infty dt e^{iEt - \eta t} \langle f_0 | \exp(-i\hat{H}t) | i_0 \rangle = \frac{1}{E_{i_0} - E} \frac{1}{E_{f_0} - E} \mathbf{v}^L \cdot \mathbf{g}(E) \cdot \mathbf{v}^R, \quad (6)$$

with  $\mathbf{g}$  the Green's function for a modified version of the bridge Hamiltonian. Specifically, it is the  $N \times N$  matrix

$$\mathbf{g}(E) = [\mathbf{H}^M - \mathbf{\Sigma}(E) - E]^{-1}, \quad (7)$$

where  $\mathbf{H}^M$  is the matrix representing the bridge Hamiltonian [Eq. (3)] and  $\mathbf{\Sigma}$  is an  $E$ -dependent "self-energy" matrix, which decomposes as

$$\mathbf{\Sigma}(E) = \mathbf{\Sigma}^L(E) + \mathbf{\Sigma}^R(E), \quad (8)$$

with elements

$$\Sigma_{I,J}^L(E) = \sum_i \frac{V_{i,I} V_{i,J}}{E_i - E - i\eta}, \quad (9)$$

and likewise for  $\mathbf{\Sigma}^R(E)$ . Furthermore, the elements of the  $N$ -d vector  $\mathbf{v}^L$  are given by  $v_I^L = V_{i_0,I}$ , and likewise for  $\mathbf{v}^R$ . The Fourier-Laplace (FL) transform given in Eq. (6) can be inverted to yield the time evolution of  $c_{f_0}(t)$

$$c_{f_0}(t) = e^{-iE_{f_0}t} \int_0^t dt' e^{i(E_{f_0} - E_{i_0})t'} \int_0^{t'} dt'' g(t' - t'') e^{iE_{i_0}(t' - t'')}, \quad (10)$$

where  $g(t)$  is the inverse FL transform of  $\mathbf{v}^L \cdot \mathbf{g}(E) \cdot \mathbf{v}^R$ , i.e.,

$$\int_0^\infty dt g(t) e^{iEt - \eta t} = \mathbf{v}^L \cdot \mathbf{g}(E) \cdot \mathbf{v}^R. \quad (11)$$

Now, if the set of L,R-reservoir states is dense, the function  $g(t)$  will decay to zero after some transient time. If the set of reservoir states is *infinitely* dense,  $g(t)$  will then remain zero for all time. If it is not, then there will be some "recurrence time" at which  $g(t)$  becomes nonzero again. However, for a sufficiently dense set of reservoir states this recurrence time can be pushed off to (almost) infinity—longer than the time scale of the experimental measurement.

So, on the "intermediate" time scale—after  $g(t)$  has decayed to zero, but before it recurs,

$$|c_{f_0}(t)|^2 = |\mathbf{v}^L \cdot \mathbf{g}(E_{i_0}) \cdot \mathbf{v}^R|^2 \frac{\sin^2[(E_{f_0} - E_{i_0})t/2]}{[(E_{f_0} - E_{i_0})/2]^2} \rightarrow 2\pi t |\mathbf{v}^L \cdot \mathbf{g}(E_{i_0}) \cdot \mathbf{v}^R|^2 \delta(E_{f_0} - E_{i_0}), \quad (12)$$

where the arrow recognizes that for sufficiently long time the factor  $\sin^2[(E_{f_0} - E_{i_0})t/2]/[(E_{f_0} - E_{i_0})/2]^2$  becomes highly peaked about  $E_{f_0} = E_{i_0}$ , with integrated strength  $2\pi t$ .<sup>17</sup>

### A. Current through the molecular wire

An important consequence of the discussion above is that the electron transfer in a (nondriven) molecular wire is *isoenergetic*. An electron with initial energy  $E_{i_0}$  can tunnel only into states in the R-reservoir with the same energy [cf. Eq. (12)]. A second important point is that the states of the metal reservoirs are all occupied below the Fermi level and unoccupied above it at temperature  $T=0$ , a condition which we assume applies in the present discussion. When the metal reservoirs are connected by a wire with no applied voltage, the Fermi levels of the L- and R-reservoirs are at the same energy. Thus tunneling from any occupied state of the L-reservoir is "blocked," because all isoenergetic states of the R-reservoir are occupied.

The situation changes when a voltage is applied across the metal contacts (reservoirs). This causes the Fermi level of the L-reservoir  $E_F^L$  to be above that of the R-reservoir,  $E_F^R$  by the amount of the applied voltage  $V_{ap}$ . Now the electrons in the L-reservoir with energy above the Fermi level of the right level can tunnel isoenergetically to the R-reservoir. We want to calculate the total rate of electron transfer (current) for a given applied voltage  $V_{ap}$ .

The overall probability to make a transition to the R-reservoir is obtained by summing  $|c_{f_0}(t)|^2$  over final states  $f_0$ . This probability is finite and proportional to  $t$ , thus establishing a well-defined transition rate  $r_{i_0}$

$$r_{i_0} \equiv \frac{1}{t} \sum_{f_0} |c_{f_0}(t)|^2 = 2\mathbf{v}^L \cdot \mathbf{g}(E_{i_0}) \mathbf{\Delta}^R(E_{i_0}) \mathbf{g}^\dagger(E_{i_0}) \cdot \mathbf{v}^L, \quad (13)$$

with  $\mathbf{\Delta}^R$  an  $N \times N$  "spectral density" matrix given by

$$[\mathbf{\Delta}^R(E)]_{I,I'} = \pi \sum_f V_{f,I} V_{f,I'} \delta(E - E_f). \quad (14)$$

Again, assuming that the temperature is sufficiently low that the  $T=0$  limit of the Fermi distribution can be invoked, the total current  $I$  is given as the sum of contributions from all incident electronic states in the range  $E_F^R < E_{i_0} < E_F^L$

$$I = \frac{2}{\pi} \int_{E_F^R}^{E_F^L} dE \text{tr} \{ \mathbf{\Delta}^L(E) \mathbf{g}(E) \mathbf{\Delta}^R(E) \mathbf{g}^\dagger(E) \}, \quad (15)$$

with

$$[\mathbf{\Delta}^L(E)]_{I,I'} = \pi \sum_i V_{i,I} V_{i,I'} \delta(E - E_i). \quad (16)$$

### III. TIGHT-BINDING MODEL OF LASER-DRIVEN MOLECULAR WIRE

Suppose that a monochromatic electric field of frequency  $\omega$  and amplitude  $\mathcal{E}_0$  is applied along the axis of the bridge molecule. Because the wavelength of light (typically in the near-IR or visible region for the problem of interest here; see below) is much longer than the dimensions of the molecular wire, we would naturally expect it to be constant at a given time over the entire spatial extent of the molecule, if the latter was “free-standing” (not attached to electrodes).

This expectation is clouded by the presence of the two metal contacts, which are also illuminated by the light. In the present work, we assume the metal contacts are perfect conductors, so that the electric field inside them is identically zero.<sup>18</sup> We further assume that the electric field imposed by radiation from the light source is not strongly disturbed in the region where the molecular wire is situated, and hence can be considered constant and equal to its free-space value here. With these assumptions, the Hamiltonian of the system is modified to  $\hat{H} \rightarrow \hat{H} - e_0 \phi^l \cos(\omega t)$ , where  $\phi^l$  is the spatially dependent electric potential established by the light source.  $\phi^l$  is taken to be zero in the left reservoir, vary linearly across the junction region (where the molecule sits), and be constant inside the right reservoir. Furthermore, its slope in the junction region is given by  $-d\phi^l/dx = \mathcal{E}_0$ , with  $x$  the direction perpendicular to the electrodes (again, we assume the electric field radiated by the light source is polarized in this direction—basically, along the molecular wire).

Thus, in the junction region, the spatial dependence of the radiated electric field takes the form  $-e_0 \phi^l = \mu \mathcal{E}_0$ , where  $\mu$  is the  $x$  component of the (negative of the) electric dipole operator:  $\mu \equiv e_0 x$ . We assume further that the electric dipole operator is diagonal in the basis of atomic orbitals (“site-orbitals”), due to the small spatial overlap between different orbitals (this overlap falls off exponentially with inter-orbital separation). Moreover, the diagonal dipole matrix elements are assumed to be given to a good approximation by the position of the site orbital (with all zeroth-order states in the L-reservoir characterized by the same position, and likewise for the R-reservoir). That is,  $\langle I | \mu | I \rangle = \mu_I = e_0 x_I$ , where  $x_I$  is the position of the  $I$ th atomic site orbital of the bridge molecule. Finally, since the electric potential is assumed to be constant in both reservoirs, we assume that  $\phi^l$  is diagonal in the reservoir states, and has the same value in all L-reservoir states, namely  $\mu_L = e_0 x_L = 0$  (taking the position of the surface of the left electrode to be at  $x=0$ ). Consequently, in the R-reservoir, the diagonal element of  $\phi^l$  implies a value  $\mu_R = e_0 x_R$ , where  $x_R$  is the position of the surface of the metal contact corresponding to the R-reservoir.

We note that to the extent that the dipole moment operator is not diagonal in the original site basis  $|I\rangle$ , one can perform an orthogonal linear transformation which renders it so. This does not compromise the essential structure of the tight-binding Hamiltonian under consideration here. Further details of this procedure will be given in Paper II.<sup>15</sup> In the present discussion, we shall assume that  $\hat{\mu}$  is “naturally di-

agonal” in the molecular bridge site basis adopted in order to specify our Hamiltonian operator.

The tight-binding Hamiltonian for a general monochromatic field-driven molecular wire then reads

$$\begin{aligned} \hat{H}(t) = & \sum_i (E_i + \mu_L \mathcal{E}_0 \cos(\omega t)) |i\rangle \langle i| + \hat{H}^M(t) \\ & + \sum_f (E_f + \mu_R \mathcal{E}_0 \cos(\omega t)) |f\rangle \langle f| \\ & + \sum_I \sum_i V_{i,I} (|i\rangle \langle I| + |I\rangle \langle i|) \\ & + \sum_I \sum_f V_{f,I} (|f\rangle \langle I| + |I\rangle \langle f|), \end{aligned} \quad (17)$$

with the (driven) bridge Hamiltonian

$$\hat{H}^M(t) = \sum_I (E_I + \mu_I \mathcal{E}_0 \cos(\omega t)) |I\rangle \langle I| + \sum_{I \neq J} V_{I,J} |I\rangle \langle J|. \quad (18)$$

As in the nondriven case, associated with this Hamiltonian is a state vector of the form indicated in Eq. (4), and the time-dependent Schrödinger equation (SE),  $i|\dot{\psi}(t)\rangle = \hat{H}(t)|\psi(t)\rangle$ , is converted into a set of first order ODE's of the form  $i\dot{c}_\alpha(t) = \sum_\beta H_{\alpha,\beta}(t)c_\beta(t)$  with  $\alpha, \beta = i, I, f$ . Furthermore, the basic dynamical problem is the same as in the zero-field case: calculate the time-evolution of a system (electron) prepared at  $t=0$  in a single state  $i_0$  of the L-reservoir.

The field-off limit of this system,  $\mathcal{E}_0=0$ , has been extensively and profitably analyzed using Green's function methods (described above). For the field-driven case, it is less obvious how to apply Green's function (GF) techniques, since these require a time-independent Hamiltonian. However, using Floquet theory,<sup>19,20</sup> the periodically time-driven Hamiltonian of interest here can be mapped to a (modified and augmented) time-independent form with the same essential structure as in the field-free case. Thus, the GF method can still be applied, and ultimately used to calculate current flow through the wire.

### IV. FLOQUET MAPPING OF FIELD-DRIVEN MOLECULAR WIRE TO AN EQUIVALENT FIELD-OFF MOLECULAR WIRE

To exploit Floquet theory in our analysis of the field-driven wire, it is useful to transform to an interaction picture (IP) with respect to the time-dependent driving terms. That is, we introduce the IP coefficients  $b_\alpha(t)$  [i.e.,  $c_I(t) = \exp[-i\mu_I \mathcal{E}_0 \sin(\omega t)/\omega] b_I(t)$ , etc.]. This removes the driving terms from the diagonal elements of the Hamiltonian and puts them into the off-diagonal ones. Specifically,

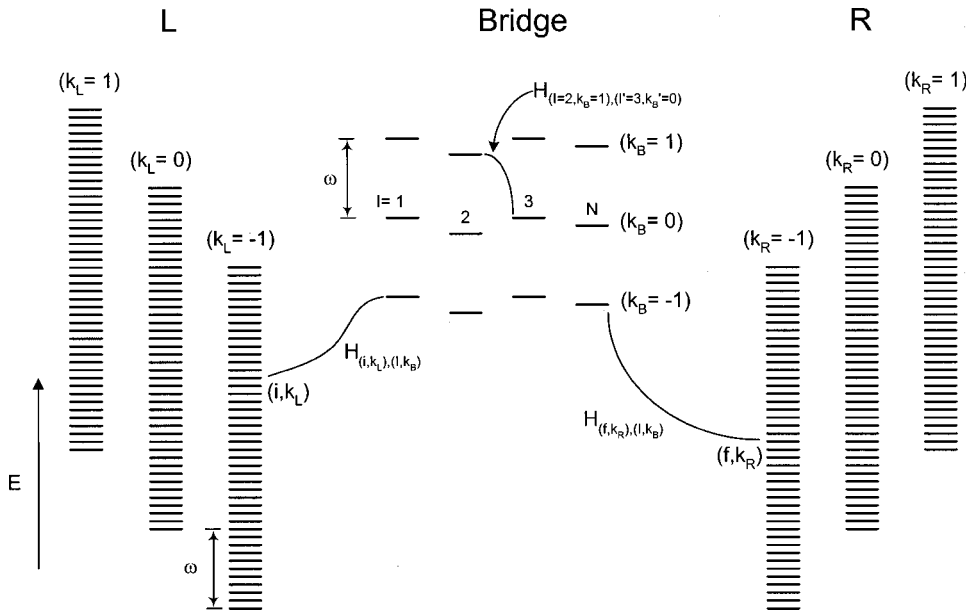


FIG. 2. Floquet state diagram for driven molecular wire system. (Site energies of the physical bridge molecule and metal states are labeled by  $k_L=0, k_B=0, k_R=0$ .)

$$\begin{aligned} \hat{H}_T(t) = & \sum_i E_i |i\rangle \langle i| + \hat{H}_T^M(t) + \sum_f E_f |f\rangle \langle f| \\ & + \sum_I \sum_i V_{i,I} (|i\rangle \langle I| e^{-ia_{iL} \sin(\omega t)} + |I\rangle \\ & \times \langle i| e^{-ia_{LI} \sin(\omega t)} + \sum_I \sum_f V_{f,I} (|f\rangle \\ & \times \langle I| e^{-ia_{iR} \sin(\omega t)} + |I\rangle \langle f| e^{-ia_{fR} \sin(\omega t)}), \end{aligned} \quad (19)$$

with the IP bridge Hamiltonian

$$\hat{H}_T^M(t) = \sum_I E_I |I\rangle \langle I| + \sum_{I \neq J} V_{I,J} |I\rangle \langle J| e^{-ia_{JI} \sin(\omega t)}. \quad (20)$$

In these expressions, the dimensionless field amplitudes  $a_{\alpha\beta}$  ( $\alpha, \beta = i, I, f$ ), are given by

$$a_{\alpha\beta} = \mathcal{E}_0 (\mu_\alpha - \mu_\beta) / \omega = -a_{\beta\alpha}, \quad (21)$$

with all  $\mu_i = \mu_L$ , and all  $\mu_f = \mu_R$ .<sup>21</sup> The IP Schrödinger then reads

$$i\dot{b}_\alpha(t) = \sum_\beta (H_T)_{\alpha,\beta}(t) b_\beta(t); \quad \alpha, \beta = i, I, f. \quad (22)$$

Following the procedure prescribed by Floquet theory, the IP Schrödinger coefficients are expanded in a Fourier series based on the periodicity of the driving field. That is,

$$b_\alpha(t) = \sum_{m=-\infty}^{\infty} b_{\alpha,m}(t) e^{im\omega t}; \quad \alpha = i, I, f. \quad (23)$$

The auxiliary Floquet coefficients  $b_{\alpha,m}$  remain to be determined. This is done by substituting Eq. (23) into the IP Schrödinger equation simultaneously with the following Fourier expansion of the driving terms appearing there<sup>12</sup>

$$e^{ia \sin \omega t} = \sum_{m=-\infty}^{\infty} J_m(a) e^{im\omega t}, \quad (24)$$

where  $J_m$  is the Bessel function of order  $m$ . Identifying the net coefficient of each  $\exp(im\omega t)$  term generates a set of coupled linear first-order ODE's for the Floquet coefficients  $b_{\alpha,m}$ . In fact, these ODE's have the form of a Schrödinger equation characterized by a time-independent Hamiltonian which nevertheless bears an intimate resemblance to the physical Hamiltonian. The Floquet Hamiltonian  $\mathbf{H}^F$  is associated with an augmented state space. For each physical state  $b_\alpha(t)$  in the physical system, there is a discrete manifold of states  $b_{\alpha,m}(t)$  in the Floquet system. In other words, in the equivalent Floquet system, there are replicas of the physical states shifted by all integer multiples of the photon quantum. These Floquet states are thus naturally labeled by two indices  $(\alpha, m)$ , where, again,  $\alpha = i, I, f$  describes the physical state which is replicated and  $m = \dots -1, 0, 1, \dots$  labels the replica number. The energy of Floquet state  $(\alpha, m)$ , referred to as a "quasienergy," in order to distinguish it from the site energies of the various physical states, is

$$E_{\alpha,m} = E_\alpha + m\omega. \quad (25)$$

Off-diagonal matrix elements in the Floquet Hamiltonian include: coupling of L-reservoir Floquet states to bridge Floquet states

$$H_{(i,k_L),(l,k_B)}^F = V_{i,l} J_{k_L - k_B}(a_{lI}), \quad (26)$$

coupling of Floquet bridge states to other Floquet bridge states

$$H_{(I,k_B),(I',k_B')}^F = V_{I,I'} J_{k_B - k_B'}(a_{II'}), \quad (27)$$

and, finally, coupling of Floquet bridge states to R-reservoir Floquet states

$$H_{(f,k_R),(l,k_B)}^F = V_{f,l} J_{k_R - k_B}(a_{fI}). \quad (28)$$

It is useful to construct a state coupling diagram for the effective field-off system generated by Floquet analysis, as is done in Fig. 2. This diagram shows clearly that the Floquet

Hamiltonian relevant to the driven system has the same generic structure as that of a *nondriven* molecular wire: Both the bridge and the reservoirs are expanded (augmented) in a straightforward manner, and the various couplings coefficients are modified, too.

To represent the physical initial condition  $b_{i_0}(0) = 1$  (all other coefficients equal 0), we will choose  $b_{i_0, k_L=0}(0) = 1$  (all other Floquet coefficients equal 0). From Fig. 2 and the details presented in the preceding paragraphs, it follows immediately that the Green's function analysis utilized in the case of the nondriven molecular wire can be applied to the Floquet Hamiltonian for the monochromatic field-driven wire.

One important aspect of the connection between the quantum dynamics obtained from the Floquet Hamiltonian and that of the corresponding physical system should be emphasized. As stressed at the outset, for a time-independent Hamiltonian of the type under consideration here, i.e., having the essential structure of Eq. (2), the principle of energy conservation holds: After short time transients, the molecule can only tunnel *isoenergetically*, i.e., such that the (quasi)energy of the final state in the R-reservoir is equal to that of the initially populated Floquet state in the L-reservoir. Relating this property to the dynamics of the underlying physical, time-driven system is aided by the following observations.

When one computes (e.g., numerically), dynamics under the time-driven Hamiltonian system prescribed by Eq. (17), it is found that an electron starting from energy level  $E_{i_0}$  can end up in the final state  $E_{f_0} = E_{i_0} + n\omega$ , where  $n$  is an integer (positive, negative, or zero), corresponding to net absorption of  $n$  photons (with negative values of  $n$  corresponding to emission). To connect the behavior of the time-independent Floquet Hamiltonian to that of the underlying time-driven system, one simply has to recognize that different isoenergetic transitions in the Floquet dynamics correspond to photon absorption–emission in the physical system (i.e., have physical final state energies that are shifted from  $E_{i_0}$  by integral multiples of the photon quantum). Transitions to the  $k_R=0$  R-reservoir replica correspond to net zero photon absorption, transitions to  $k_R=1$  correspond to net one-photon emission, etc., or, equivalently, a transition from an L-reservoir state with energy  $E_{i_0}$  to an R-reservoir state with energy  $E_{i_0} + n\omega$  corresponds in the Floquet picture to an isoenergetic transition (at energy  $E_{i_0}$ ) from L-reservoir replica  $k_L=0$  to R-reservoir replica  $k_R=-n$ . In this way the currents associated with electrons arriving at the various allowed final state energies in the field-driven system can be quantitatively accounted for via Floquet analysis.

Finally, we discuss the issue of how to truncate the formally infinite manifold of Floquet states. Fortunately, the principle of “state mixing,” i.e., that two zeroth-order states couple more strongly if they are nearly degenerate than if they are not, assures that only Floquet replicas which are nearly iso-energetic with  $E_{i_0}$  need be retained. In practice we keep the few “most nearly degenerate” Floquet reservoir and bridge replicas and ignore the rest. The number of replicas is expanded until numerical convergence is attained. Typically,

the number of replicas which must be retained is modest—examples are given in Sec. VI.

## V. AN “INDEPENDENT CHANNEL APPROXIMATION” TO FIELD-DRIVEN TRANSPORT

The mapping of the time-driven Hamiltonian given in Sec. IV via Floquet theory to a time-independent Hamiltonian with the same form as the canonical (non-driven) tight-binding molecular wire Hamiltonian is precise, and thus leads to a precise way to calculate current flow through a laser-driven molecular wire. As described in Sec. IV, the effective system generated by the Floquet mapping has an augmented bridge comprising  $N_b N$  sites, where  $N$  is the number of sites in the physical bridge molecule and  $N_b$  is the number of Floquet bridge replicas retained in the calculation. Associated with this augmented bridge is a Floquet bridge Hamiltonian and a Floquet self-energy matrix (the latter being a function of the parameter  $E$ ). The linear dimension of both matrices is  $N_b N$ , where the value of  $N_b$  is formally infinity, though in practice convergence can be obtained with a finite and often modest value (corresponding to  $N_b$  replicas), as noted above. Nevertheless, as the calculation gets more complicated, physical insight can become obscured.

Some insight can be restored by considering an approximation, to be termed the Independent Channel Approximation (ICA), in which off-diagonal terms coupling different Floquet replicas in the  $N_b N$  augmented bridge Hamiltonian and self-energy are neglected. This renders both matrices block diagonal with an  $N \times N$  block representing each Floquet replica. Consequently, the Green's function attains the same block diagonal structure.

We denote the self-energy modified bridge Green's function associated with the Floquet Hamiltonian as  $\mathbf{g}^F(E)$ . It has the structure indicated in Eq. (7), bearing in mind that the appropriate bridge Hamiltonian is the augmented (multireplica) version depicted schematically in Fig. 2: thus  $\mathbf{g}^F$  is an  $N_b N \times N_b N$  matrix. Similarly, the appropriate L- and R-reservoirs which determine the self-energy matrix that enters into  $\mathbf{g}^F$  are the multireplica versions also depicted in Fig. 2. [The coupling elements connecting sites of the extended bridge to states of the extended reservoirs are specified in Eqs. (26)–(28).] Formally, an infinite number of reservoir replicas has to be considered, but in practice the number of contributing replicas is modest because  $|J_n(a)| \rightarrow 0$  as  $n \rightarrow \infty$  (for fixed  $a$ ). The elements of  $\mathbf{g}^F$  are explicitly prescribed in Appendix A.

In general, the transition probability for an initial state  $i_0$  of the L-reservoir to a final state  $f_0$  of the R-reservoir which is nearly on-resonance with a net  $N_p$ -photon emission (corresponding in the Floquet Hamiltonian system to transitions to the R-reservoir replica  $k_R = N_p$ ) is

$$|b_{f_0}(t)|^2 \cong 2\pi t \delta(E_{f_0} + N_p \omega - E_{i_0}) |\mathbf{v}^L \cdot \mathbf{g}^F(E_{i_0}) \cdot \mathbf{v}^R|^2, \quad (29)$$

with the  $N_b N$  dimensional array  $\mathbf{v}^L$  consisting of the coupling elements

$$V_{i_0, I} J_k(a_{IL}); \quad I=1,2,\dots,N, \quad k=1,2,\dots,N_b.$$

Similarly,  $\mathbf{v}^R$  consists of elements  $V_{f_0, I} J_{N_p - k}(a_{RI})$ .

As noted above, within the ICA the Green's function  $\mathbf{g}^F$  becomes block diagonal, each block having the linear dimension  $N$  of the physical molecular bridge. Thus, the ICA implies

$$\mathbf{v}^L \cdot \mathbf{g}^F(E_{i_0}) \cdot \mathbf{v}^R \cong \sum_{k_L=-\infty}^{\infty} \mathbf{v}_{k_L}^L \cdot \mathbf{g}^{\text{eff}}(E_{i_0} - k_L \omega) \cdot \mathbf{v}_{N_p - k_L}^R. \quad (30)$$

The matrix  $\mathbf{g}^{\text{eff}}$  on the r.h.s. of this expression is an effective molecular Green's function. It has the dimensions of the physical bridge, i.e.,  $N \times N$ , and also the same generic structure as in the field-off case, namely

$$\mathbf{g}^{\text{eff}}(E) = (\mathbf{H}_{\text{eff}}^M - \Sigma^{\text{eff}}(E) - E)^{-1}. \quad (31)$$

In this expression,  $\mathbf{H}_{\text{eff}}^M$  is an effective molecular bridge Hamiltonian matrix, dimension  $N \times N$ . Its diagonal elements are the bridge site-energies  $E_I$  and its off-diagonal elements are renormalized bridge coupling parameters  $V_{II'} J_0(a_{II'})$ . The corresponding effective  $N \times N$  effective self-energy matrix  $\Sigma^{\text{eff}} = \Sigma^{L, \text{eff}} + \Sigma^{R, \text{eff}}$  is defined as

$$\Sigma_{I, J}^{L, \text{eff}}(E) = \sum_{m=-\infty}^{\infty} J_m(a_{LJ}) J_m(a_{LJ}) \Sigma_{I, J}^L(E - m\omega), \quad (32)$$

$\Sigma^L$  being the left reservoir spectral density of the physical (field-off) wire, as prescribed in Eq. (9); and analogously for  $\Sigma^{R, \text{eff}}(E)$ . Finally, the elements of the  $N$ -dimensional vectors  $\mathbf{v}_k^{L, R}$  are given by

$$(\mathbf{v}_k^L)_I = V_{i_0, I} J_k(a_{IL}); \quad (\mathbf{v}_k^R)_I = V_{f_0, I} J_k(a_{RI}).$$

The decomposition provided by the ICA enables more rapid numerical evaluation because of its "divide and conquer" flavor. In particular, the size of the matrices which have to be inverted is greatly reduced (particularly for large  $N_b$ ). However, the primary utility of the channel decomposition is that it provides a way to anticipate the origin of large contributions to the current by associating individual contributions to Eq. (30) with specific electron transfer pathways or "channels." This interpretation is discussed next, as is the expected regime of validity of the ICA.

### A. Interpretation and validity regime of the independent channel picture

Each term on the right-hand side (rhs) of Eqs. (30) can be described as the probability amplitude for the electron to make a transition from  $i_0$  of the left reservoir to  $f_0$  of the R-reservoir in three steps, namely: (i) emission of  $k_L$  photons to access the molecular bridge from the L-reservoir (controlled by the term  $\mathbf{v}_{k_L}^L$ ), (ii) isoenergetic tunneling across the bridge, i.e., at energy  $E_{i_0} - k_L \omega$  [controlled by the term  $\mathbf{g}^{\text{eff}}(E_{i_0} - k_L \omega)$ ], and finally (iii) emission of  $N_p - k_L$  photons in the transition from the bridge to the R-reservoir (controlled by the term  $\mathbf{v}_{N_p - k_L}^R$ ). Typical channels are depicted schematically in Fig. 3. The product of the three factors just delineated determines the amplitude for the process de-

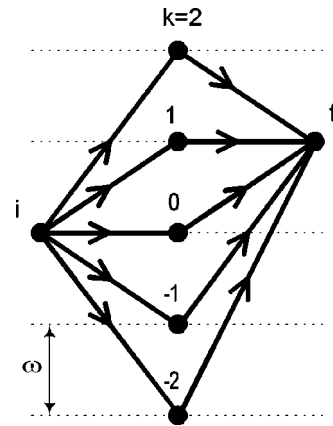


FIG. 3. Schematic illustration of net one-photon absorption pathways through a molecular bridge in the Independent Channel Approximation.

scribed. Each integer value of  $k_L$  defines a distinct channel, and the contribution from all channels must be included in the sum (at the amplitude level).

The rationale behind this interpretation is straightforward. The term  $J_k$  is associated with  $k$ -photon emission. Thus the factor  $\mathbf{v}_{k_L}^L$  connects the L-reservoir to the bridge (via  $k_L$  photon emission) and the factor  $\mathbf{v}_{N_p - k_L}^R$  connects the bridge to the R-reservoir (via  $N_p - k_L$  photon emission). Note further the properties of the effective molecular bridge Green's function  $\mathbf{g}^{\text{eff}}(E)$ . The site energies of  $\mathbf{H}_{\text{eff}}^M$  are just the site energies of the bridge molecule, while the hopping elements are the physical bridge hopping elements slightly modified by an appropriate factor of  $J_0$ . Usually we will have  $a_{II'} \ll 1$  for site orbitals which are connected by large values of  $V_{II'}$ . Thus, the effective molecular bridge closely resembles the physical bridge, and in particular the molecular orbital (MO) energies are close to the physical bridge MO's. Consequently, resonances in  $\mathbf{g}^{\text{eff}}(E)$  reflect the MO energies of the bridge molecule. In particular, the amplitude (ii) for isoenergetic tunneling through the bridge will be significant when  $E_{i_0} - k_L \omega$  is approximately equal to an MO energy of the bridge, that is, when emission of  $k_L$  photons brings the energy of the tunneling electron into resonance with one of the MO's of the bridge. This interpretation is particularly easy to appreciate in the special, but conceptually important, case that the L-reservoir couples only to the orbital  $I=1$  of the bridge (located closest to the left electrode), and the R-reservoir couples only to the orbital  $I=N$  (located closest to the right electrode). In this case the ICA transition rate formulas simplify considerably, as discussed in Appendix B.

We should stress that this picture of independent electronic channels or pathways between the left and right metallic contacts is an approximate one, being predicated on the neglect of off-diagonal matrix elements in the Floquet Green's function which couple different Floquet bridge replicas. It will be thus be most accurate when electronic coupling matrix elements are small, the laser-field is weak, or there is a large energy gap between the quasi-energies of different bridge replicas arising from a high photon frequency. In the first two circumstances the elements of the inter-replica coupling blocks go to zero, while in the third

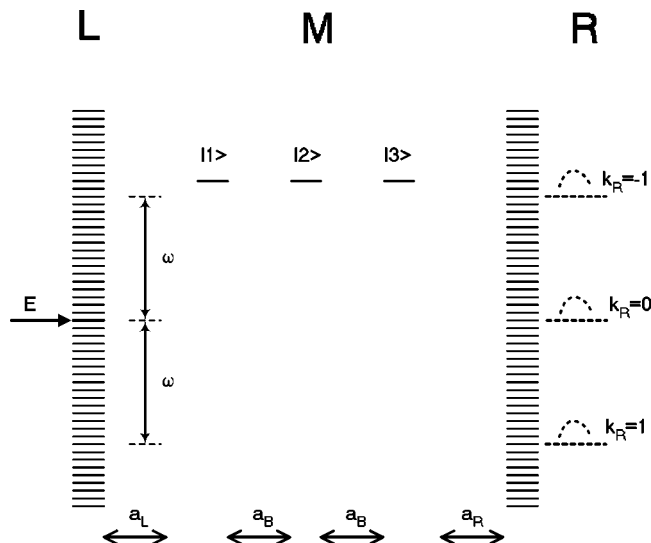


FIG. 4. Schematic representation of a molecular wire system corresponding to a 3 state molecular bridge. “Blips” associated with  $k_R=0, \pm 1$  depict allowed final state energy regimes for the indicated laser frequency. See text for further details.

there is poor “mixing” between the zeroth-order states in separate replicas due to the large gaps between their zeroth-order (quasi)energies. The best way to ensure that the ICA is valid is to correct it by coupling several bridge replicas together and verifying that the effects of such coupling are small.

Another way to include inter-replica coupling is to carry out a perturbation expansion<sup>16</sup> of the generic form:  $G = G_0 - G_0 V G_0 + G_0 V G_0 V G_0 - \dots$ , where  $G$  here is the full Floquet Green’s function,  $G_0$  is the block diagonal part of this and  $V$  is the off-diagonal, inter-replica coupling part of the full Floquet Hamiltonian which is neglected in  $G_0$ . For sufficiently small  $V$ , this expansion is convergent, and in such cases, it provides insight by enumerating possible pathways for electron transport across the bridge. The  $G_0$  term (ICA approximation) corresponds to photon absorption–emission only between L-, R-reservoirs and the bridge (no photon absorption–emission as the electron hops between bridge states), while the  $G_0 V G_0$  term adds in processes that include one photon absorption–emission within the manifold of bridge states, etc. A full description of this expansion, its range of validity, and insights that can be gleaned from it will be presented elsewhere.<sup>22</sup>

As noted above, we have opted in the present work to include inter-replica coupling effects by performing basis set inversion with an expanded number of bridge Floquet replicas. The basis set method, when convergence can be obtained (which we have found to be the case here), avoids any potential errors encountered in truncating the perturbation expansion at some finite and often low order.

## VI. RESULTS FOR A MODEL SYSTEM

In this section we present numerical results for a simple model system. Our goal is to illustrate the features of the underlying quantum dynamics of monochromatic field-assisted electron transport in a molecular electron transfer

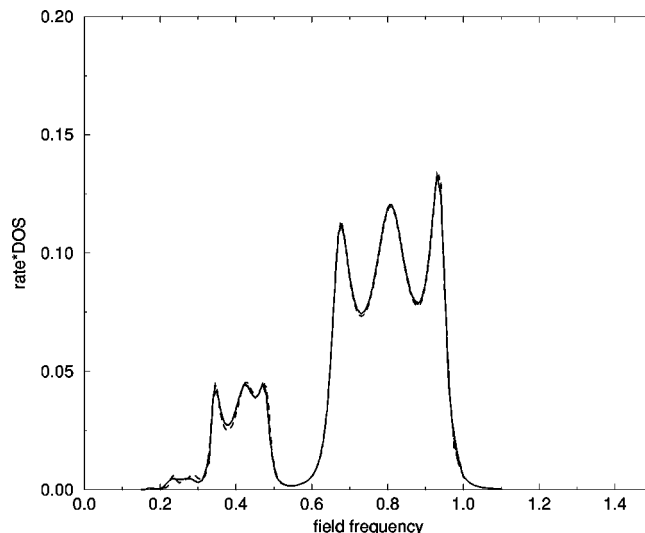


FIG. 5. Rate of transitions to the R-reservoir of an electron initially prepared in state  $E=0$  of the L-reservoir as a function of the laser field frequency. [In this and subsequent figures, transition rates to the R-reservoir from an incident electron at  $E=0$  of the L-reservoir are scaled by the density of states (DOS) at this energy.] Results obtained from integration of the Schrödinger equation for the (physical) time-driven system are shown via the dashed line. Corresponding results obtained by direct integration of (time-independent) Floquet Hamiltonian are shown via the solid curve. Results obtained from the Floquet Green’s function analysis presented in the text are indistinguishable from the solid curve. The following parameters were utilized:  $a_B=0.1$ ,  $V_B=0.1$ ,  $a_{L,R}=2$ ;  $V_{ap}=0$ .

system attached to metallic reservoirs. We do not attempt to extract “realistic” current-voltage characteristics here. This will be done in a subsequent paper.<sup>15</sup> Thus, our model consists of a symmetric three-site molecule coupled symmetrically to left and right metallic reservoirs of finite energetic width, as sketched in Fig. 4. The reservoir states span the energy regime  $-1 < E < 1$ . All three bridge site energies are taken to have the same value, namely  $E_B=0.8$ —thus they lie within the reservoir energy band.<sup>23</sup> We assume only nearest-neighbor electronic coupling between orbitals in the bridge Hamiltonian. Furthermore, only bridge state 1 interacts with the L-reservoir, and only bridge state 3 interacts with the R-reservoir. The strength of the bridge-electrode interaction and reservoir density of states is prescribed by the Newns–Anderson spectral density

$$\Delta(E) = \frac{V^2}{\gamma} \sqrt{1 - (E/2\gamma)^2}, \quad |E/2\gamma| < 1, \quad (33)$$

where  $V^2/\gamma=0.12$  and  $\gamma=0.5$ . We choose driving field parameters such that the reservoir-bridge field parameter  $a_{L,R}=2$  throughout, with the parameters  $a_L \equiv a_{1,L}$  and  $a_R \equiv a_{3,R}$  [cf. Eq. (21) above]. For simplicity, and to focus on consequences of the driving field, we set the applied static electric field to zero (i.e., no modification of the one-electron orbital site-energies by a static applied voltage).

In the calculations presented below, we consider the dynamics of an *isolated* electron according to the one-electron Hamiltonian 17. To illustrate how solutions to this time-dependent Schrödinger equation can be obtained using the approach developed in the previous sections, we ignore effects due to the presence of other electrons in the reservoirs,

including the exclusion of the tunneling electron from any occupied R-reservoir state. Clearly, such effects have to be included in any complete calculation of current through a molecular wire attached to electrodes. We defer this important exercise to Paper II.<sup>15</sup>

Figure 5 shows the rate of transitions to all states of the R-reservoir for a system prepared initially in an  $E=0$  state of the L-reservoir, for driving-field parameter choices  $a_B=0.2$ , where  $a_B \equiv a_{2,1} = a_{3,2}$ , and intra-bridge coupling  $V_B=0.1$ . (Again, we fix the value  $a_{L,R}=2$  in all results presented in this section, and we have set the applied static bias  $V_{\text{ap}}=0$ .) Three different calculations are displayed. The dashed line shows the result obtained by direct integration of the time-dependent field-driven Schrödinger equation. In practice, this was done by representing the left and right electronic reservoirs using a finite set of states, evenly spaced in energy, and coupled to the bridge via matrix elements  $V_{i,1}$  and  $V_{f,N}$  [cf. Eq. (2)] selected in accordance with the spectral densities  $\Delta^{(L,R)}$ . [The formal definition of the spectral densities was given in Eqs. (14) and (16), and the specific functional form in Eq. (33) above.] Convergence was obtained by increasing the number of discrete states in the reservoirs, while maintaining the desired (finite) spectral density by reducing the individual reservoir-bridge coupling elements accordingly.

The solid line in Fig. 5 shows the result of direct numerical integration of the time-independent Floquet Hamiltonian, keeping six bridge replicas (specifically,  $k_B = -4 \cdot 1$ ) and seven L- and R-reservoir replicas (specifically,  $k_{L,R} = -3 \cdot 3$ ). [The discretization of the reservoir continua outlined in the previous paragraph was employed here, too.] This result is identically reproduced to within the resolution of the figure by the Green's function formula recorded in Sec. II, as implemented for the Floquet Hamiltonian described in Sec. IV, including the same range of reservoir replicas in the calculation of the relevant self-energies (cf. Appendix A). The agreement between direct simulation of the time-driven system and computations based on the Floquet mapping to an effective time-independent system is seen to be quite good. Moreover, the Green's function analysis of the dynamics of the (time-independent) Floquet Hamiltonian system is completely satisfactory. Thus, in the remainder of the numerical studies to be presented in this work we will simply use the Green's function formulas to obtain transition rates from the left to the right reservoirs through the molecular bridge.

Before considering other examples, it is worthwhile to study the results portrayed in Fig. 5 in more detail. In these plots, the transition rate to the R-reservoir is scanned as a function of laser frequency, holding the laser intensity parameters  $a_{L,R}$  and  $a_B$  fixed.<sup>24</sup> The shape of the spectrum thus generated reflects the details of the molecular bridge Hamiltonian. In particular, as discussed above, the molecular Green's function has *resonances* at the values of the molecular orbital energies. In the present example, the molecular orbital energies of the bridge are far from the incident energy of the electron in the L-reservoir. Thus, in the absence of the applied laser field, the electron transport (tunneling) is extremely weak. However, by absorbing (or in the general case,

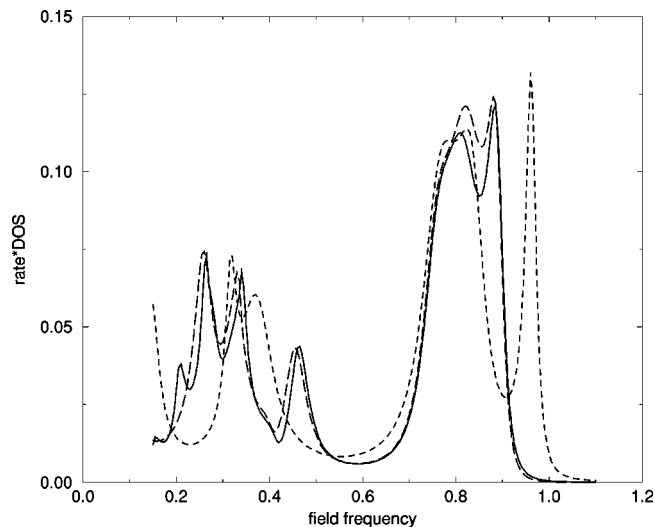


FIG. 6. Dependence of the current vs frequency curve on the number of Floquet replicas in the Floquet Hamiltonian. Solid line shows results with (10,9) (bridge, reservoir) replicas (see text for full details). Long-dashed line shows corresponding result for (6,7); short-dashed line shows corresponding result for (3,5). The following parameters were utilized:  $a_B=2.0$ ,  $V_B=0.5$ .

emitting) an integral number of photons, the energy of the tunneling electron is boosted by the appropriate multiple of the photon quantum. This can bring it into resonance with the molecular orbitals of the bridge Green's function and thus dramatically enhance the Green's function transmission factor. In the system studied in Fig. 5, the energy difference between the incident electron and the center of the bridge molecule molecular orbital energy level distribution is 0.8. Thus, the triplet of peaks at  $\sim \omega=0.8$  is due to one-photon absorption by the incident electron. The triplet of peaks at  $\sim \omega=0.4$  corresponds to two-photon absorption resonance, while that at  $\sim \omega=0.27$  corresponds to a three-photon absorption resonance.

The number of Floquet replicas needed to obtain good agreement with the (physical) time-driven system dynamics depends on the intra-bridge field parameter  $a_B$  and coupling matrix elements  $V_B$ . In Fig. 6 we present calculations in which the relatively large parameters  $a_B=2$  and  $V_B=0.5$  are used. In this case, a larger number of Floquet bridge and reservoir replicas (10 and 9, respectively) are needed to accurately model the field-on curve, specifically  $k_B = -6 \cdot 3$  and  $k_{L,R} = -4 \cdot 4$ .

A Green's function calculation utilizing this number of replicas is shown via the solid line. The long-dashed curve shows the results of a Green's function calculation for a Floquet Hamiltonian with a smaller number of replicas, specifically 6 for the bridge ( $k_B = -4 \cdot 1$ ) and 7 for the reservoirs ( $k_{L,R} = -3 \cdot 3$ ). Using an even smaller number of Floquet replicas, namely 3 for the bridge ( $k_B = -2 \cdot 0$ ) and 5 for the reservoirs ( $k_{L,R} = -2 \cdot 2$ ) produces an even less accurate result, indicated by the short-dashed line.

When the applied laser field is weak (hence all  $a$ -parameters are small), or the electric coupling matrix elements are small, we can approximately set nondiagonal blocks of the Floquet Green's function to zero, i.e., invoke the Independent Channel Approximation. In the ICA, once

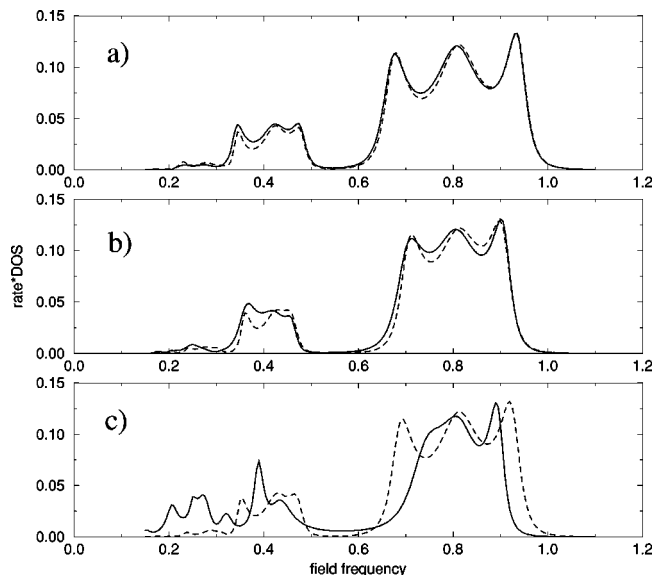


FIG. 7. Illustration of the range validity of the independent channel approximation (ICA) for different values of intra-bridge field parameter. In each panel, the solid line shows exact result for transition rate to the R-reservoir vs laser frequency; dashed line shows corresponding result within the ICA. Panel (a):  $a_B=0.2$ ,  $V_B=0.1$  (weak coupling); panel (b):  $a_B=1.0$ ,  $V_B=0.15$  (intermediate coupling); panel (c):  $a_B=2.0$ ,  $V_B=0.5$  (strong coupling).

an electron “hops” from the L-reservoir to a particular bridge replica, it then transfers between states of the same replica until it reaches the R-reservoir. The total rate of electron transfer is the sum (at the amplitude level) of contributions from all such channels.

In Fig. 7 we test the accuracy of the ICA by comparing molecular wire systems with different intra-bridge field parameters. The system is the same as that considered in Fig. 5 except for the values of  $a_B$  and  $V_B$ , which are varied as follows. In the top panel, which is characterized by an intra-bridge field parameter  $a_B=0.2$  and intra-bridge coupling  $V_B=0.1$  (both of which are small), the agreement between the exact (solid line) and ICA (dashed line) results is good. The bottom panel shows results for the same system, but with a large intra-bridge field parameter  $a_B=2$  and intra-bridge coupling strength  $V_B=0.5$ —here the agreement between the exact and approximate curve is poor. The middle panel shows results for an intermediate case, where  $a_B=1$  and  $V_B=0.15$ . The results presented in Fig. 7 demonstrate that under appropriate conditions (*vide supra*) the ICA is valid and useful.

In Fig. 8, for the same molecular wire system considered in Fig. 5, we decompose the total current to the right electrode (thick solid line) into contributions to various right reservoir Floquet replicas. The dotted line represents the current to the right electrode replica  $k_R=0$ , i.e., direct tunneling in the physical system with no net absorption–emission of photons. The long dashed line is the current to the replica  $k_R=1$  (corresponding to accumulation of electrons at an energy one photon below the tunneling electron energy; cf. Fig. 4), and the short-dashed line is the current to the replica  $k_R=-1$  (corresponding to electron accumulation at an energy one photon above the tunneling electron energy). Note that

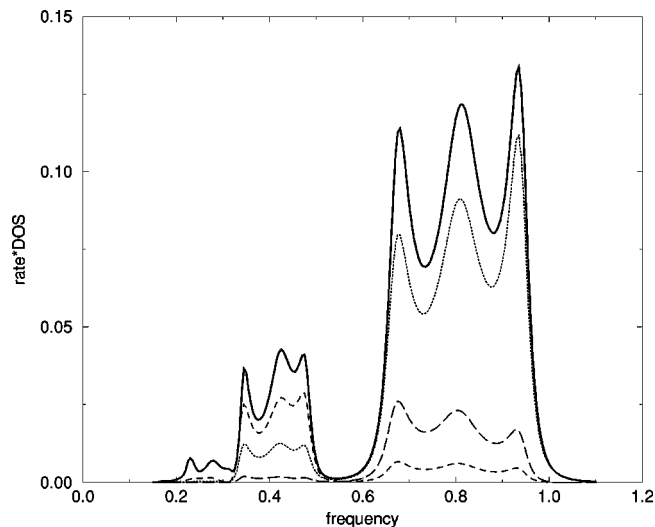


FIG. 8. Contribution of  $0, \pm 1$  net photon absorption processes to overall rate of transitions to R-reservoir. Dotted line corresponds to  $N_p=0$ , long-dashed line to  $N_p=1$  and short-dashed line to  $N_p=-1$ . The total transition rate (obtained by summing over contributions from all open channels) is indicated by the solid line. System parameters are the same as considered in Fig. 5.

the relative weights of the contributions of the  $N_p = \pm 1, 0$  channels change for the 1 versus 2 photon absorption resonance portions of the spectrum. These weights are readily explained by the exposition contained in Appendix B. For the one-photon absorption resonance region near  $\omega=0.8$ , the dominant term in the ICA rate formula is  $k_l=-1$ . Thus, since  $\Delta_R$  is a weakly varying function of energy within the region  $-1 < E < 1$ , the relative intensities of the  $N_p=1, 0, -1$  peaks is approximately  $J_2^2(2), J_1^2(2), J_0^2(2)$ , respectively. On the other hand, for the two-photon absorption portion resonance part of the spectrum in the region  $\omega \cong 0.4$ , the ratio of these peaks is approximately given by  $J_3^2(2), J_2^2(2), J_1^2(2)$ .

In the case of the one-photon absorption resonance at  $\omega=0.8$ , the  $k_R=0, \pm 1$  channels are the only ones possible. (Other values of  $k_R$  correspond to final state energies outside the energetic width of the R-reservoir.) Thus, in this portion of the spectrum the sum of the intensities for  $k_R=0, \pm 1$  processes adds up to the total intensity (solid line). For two and higher photon absorption resonances, there are other (undisplayed) open final state channels besides  $k_R=0, \pm 1$ . Thus, the  $k_R=0, \pm 1$  intensities shown in Fig. 8 do not sum to the total intensity in these parts of the spectrum.

## VII. DISCUSSION AND CONCLUSIONS

In this paper we have considered the effect of monochromatic light on transport of electrons through molecular wires. As has been done before in the field-off limit,<sup>8,9</sup> we adopted a tight-binding model of the electron transport, neglecting complications due to disorder, dissipation, electron correlation, etc. Of course these complications should be incorporated as the theory is developed further, but again, following the success of nondissipative tight binding models in de-

scribing I-V curves for “standard” (i.e., not laser-driven) molecular wires, we expect that the same level of description will be useful in the field-driven case.

In the absence of external driving, the current-voltage characteristics of nondissipative tight binding models of electron transport through molecular wires can be profitably analyzed via a Green’s function scattering approach.<sup>8,9</sup> We have shown in this work, using Floquet theory, that in the case of the field-driven analog (generated experimentally by illuminating the wire–electrode system with a monochromatic laser), the relevant time-dependent Hamiltonian can be mapped to a time-independent Hamiltonian in an extended state space and with modified interstate couplings. The modified/augmented Floquet Hamiltonian has the same essential structure as its field-off analog, and so the Green’s function analysis can be directly employed to analyze the quantum dynamics of the Floquet system. This dynamics can then be converted to dynamics of the physical (time-driven) system.

Our Floquet analysis is formally exact, and in practice can be numerically converged with a relatively modest effort. We also presented an approximate analysis, premised on certain weak-coupling assumptions which are clearly set forth above. In this approximation, the numerical effort is further reduced, and, more importantly, insight is provided into the “channels” of multiphoton absorption–emission which contribute strongly to current flow through a wire with particular molecular characteristics under given experimental conditions (applied static voltage, amplitude and frequency of the light source, etc.). We stress that this channel picture should be used as a guide, but when in doubt the full Floquet treatment should be carried out to numerical convergence.

Some prototypical illustrations of the theory and methodology were provided in the present work. We stopped short of calculating I-V curves for a “real” molecular wire (treated at the nondissipative tight binding level). Such an analysis requires considerable effort, including careful examination of the molecular electronic structure of the molecular bridge, the metal electrodes and the coupling between them. This will be described in a subsequent publication.<sup>15</sup> The goal of such a calculation, from the point of view of outlining a design principle for significantly enhancing (and ultimately, controlling) electron transport through molecular wires, is to demonstrate how the laser illumination with a *cw* light source of an appropriate frequency can convert non-resonant tunneling processes into resonant ones (by absorption or emission of photons to “boost” the tunneling electron to an energy where there are molecular orbital energies to assist tunneling through the bridge), thus dramatically enhancing the electron tunneling rate. Clearly, the smaller the laser power needed to do this, the more robust the control scheme will be. These important issues will also be addressed in Paper II.

## ACKNOWLEDGMENTS

We thank Professor A. Nitzan for several helpful conversations concerning this work. Work at the University of Pittsburgh was supported in part by National Science Foundation

grant EEC0085480. Many of the computations reported here were carried out at the University of Pittsburgh’s Center for Molecular and Materials Science.

## APPENDIX A: ELEMENTS OF THE FLOQUET GREEN’S FUNCTION MATRIX

Even after “integrating out” the reservoir states, the dimension of the Floquet Green’s function matrix  $\mathbf{g}^F(E)$  is formally infinite, since the number of bridge replicas is infinite. If  $N_b$  bridge replicas are retained explicitly, this matrix has finite linear dimension  $N_b N$ . Its elements are given by inverting the appropriate  $N_b N$  dimensional matrix:

$$\mathbf{g}^F(E) = [\mathbf{H}_M^F - \bar{\Sigma} - E]^{-1}, \quad (\text{A1})$$

where  $\mathbf{H}_M^F$  is an  $N_b N$  dimensional matrix whose elements are prescribed by Eqs. (25)–(28) in the text. Furthermore, the  $N_b N$  dimensional Floquet self-energy matrix  $\bar{\Sigma}$  is the sum of contributions from *L* and *R* electrodes

$$\bar{\Sigma}(E) = \bar{\Sigma}^L(E) + \bar{\Sigma}^R(E),$$

where

$$\bar{\Sigma}_{(I,k_B),(J,k'_B)}^L(E) = \sum_{k_L=-\infty}^{\infty} J_{k_L-k_B}(a_{LI}) J_{k_L-k'_B}(a_{LJ}) \times \Sigma_{I,J}^L(E - k_L \omega),$$

with  $\Sigma^L$  being the (laser-field off) molecular L-reservoir self-energy;  $\bar{\Sigma}^R$  is defined analogously.

It is instructive to comment on the sources of coupling that link the  $N \times N$  blocks of the inverse Floquet Green’s function matrix. First (type i), there are off-diagonal elements of  $\mathbf{H}_M^F$ , namely  $V_{I,I'} J_{k_B-k'_B}(a_{II'})$  with  $k_B \neq k'_B$ . Such terms can only couple different bridge base states (since  $V_{I,I} = 0$ ). Inter-channel coupling (type ii) is also provided by self-energy matrix elements, noted above, with  $k_B \neq k'_B$ . Coupling between the same bridge basis state in different Floquet replicas is accomplished by these terms. Note that both types of coupling vanish as the laser intensity tends to zero. Also, small intra-bridge elements  $V_{I,I'}$  and small reservoir-bridge coupling elements  $V_{i,I}$ ,  $V_{f,I}$  suppress type i and ii coupling, respectively. Finally, all other terms being equal, increasing the laser frequency  $\omega$  (with a concomitant increase in the laser amplitude to keep all *a* parameters constant) also suppresses interchannel coupling, since the diagonal matrix elements of different  $N \times N$  diagonal blocks of that comprise each channel in  $\mathbf{H}_M^F$  are separated by multiples of the laser quantum.

## APPENDIX B: PHOTON EMISSION RATES FOR THE CASE OF MINIMAL RESERVOIR–BRIDGE COUPLING

When only bridge orbital 1 couples to the L-reservoir and only bridge orbital *N* couples to the R-reservoir, the ICA transition probability formulas simplify considerably. In this case we can employ simplified notation:  $V_{i_0} = V_{i_0,1}$ ,  $V_{f_0} = V_{f_0,N}$ ,  $a_L = a_{1,L}$ ,  $a_R = a_{R,N}$ . Then, for net  $N_p$  photon emission

$$|b_{f_0}(t)|^2 \cong 2\pi t \delta(E_{f_0} + N_p \omega - E_{i_0}) V_{i_0}^2 V_{f_0}^2 \times \left| \sum_{k_L=-\infty}^{\infty} J_{k_L}(a_L) g_{1N}^{\text{eff}}(E_{i_0} - k_L \omega) J_{N_p - k_L}(a_R) \right|^2. \quad (\text{B1})$$

Then the rate of  $N_p$  photon emission  $R_{i_0} \equiv [\sum_{f_0}' |b_{f_0}(t)|^2]/t$ , where the prime on the sum indicates restriction to the local energy region near  $E_{f_0} = E_{i_0} - N_p \omega$ , is given by:

$$R_{i_0} = 2V_{i_0}^2 \Delta_R(E_{i_0} - N_p \omega) \times \left| \sum_{k_L=-\infty}^{\infty} J_{k_L}(a_L) g_{1N}^{\text{eff}}(E_{i_0} - k_L \omega) J_{N_p - k_L}(a_R) \right|^2. \quad (\text{B2})$$

A particularly important situation is when the laser is tuned into  $-k_l$  photon absorption resonance with the molecular orbital energies of the bridge. In this case the  $k_L = k_l$  term dominates in the above sums, and we can approximate

$$R_{i_0} \cong 2V_{i_0}^2 \Delta_R(E_{i_0} - N_p \omega) J_{k_l}^2(a_L) \times |g_{1N}^{\text{eff}}(E_{i_0} - k_l \omega)|^2 J_{N_p - k_l}^2(a_R). \quad (\text{B3})$$

Of course, the validity of this formula requires a laser intensity such that  $J_{k_l}^2(a_L) \neq 0$  and  $J_{N_p - k_l}^2(a_R) \neq 0$ .

<sup>1</sup>C. Joachim, *New J. Chem.* **15**, 223 (1991).

<sup>2</sup>See, for example, *Atomic and Molecular Wires*, edited by Christian Joachim and Siegmund Roth, (Kluwer Academic, Dordrecht, 1997).

<sup>3</sup>G. Leatherman, E. N. Durantini, D. Gust, T. A. Moore, A. L. Moore, Z. Zhou, P. Rez, Y. Z. Liu, and S. M. Lindsay, *J. Phys. Chem. B* **103**, 4006 (1999).

<sup>4</sup>See, for example, *Molecular Electronics*, edited by M. A. Ratner and J. Jortner (Butterworth, London, 1997).

<sup>5</sup>M. A. Reed, C. Zhou, C. J. Muller, T. P. Burgin, and J. M. Tour, *Science* **278**, 252 (1997).

<sup>6</sup>S. Datta, *Electronic Transport in Mesoscopic Systems* (Cambridge University Press, Cambridge, 1995).

<sup>7</sup>B. J. Keay, S. Zeuner, S. J. Allen, Jr., K. D. Maranowski, A. C. Gossard, U. Bhattacharya, and M. J. W. Rodwell, *Phys. Rev. Lett.* **75**, 4102 (1995).

<sup>8</sup>V. Mujica, M. Kemp, and M. A. Ratner, *J. Chem. Phys.* **101**, 6849 (1994); **101**, 6856 (1994).

<sup>9</sup>M. P. Samanta, W. Tian, S. Datta, J. I. Henderson, and C. P. Kubiak, *Phys. Rev. B* **53**, R7626 (1996); W. Tian, S. Datta, S. Hong, R. Reifengerger, J. I. Henderson, and C. P. Kubiak, *J. Chem. Phys.* **109**, 2874 (1998); S. Datta, W. Tian, S. Hong, R. Reifengerger, J. I. Henderson, and C. P. Kubiak, *Phys. Rev. Lett.* **79**, 2530 (1997).

<sup>10</sup>C. Joachim and J. Vinuesa, *Europhys. Lett.* **33**, 635 (1996).

<sup>11</sup>N. D. Lang, *Phys. Rev. B* **52**, 5335 (1995); M. Di Ventura, S. T. Pantelides, and N. D. Lang, *Phys. Rev. Lett.* **84**, 979 (2000).

<sup>12</sup>Y. Dakhnovskii and R. Coalson, *J. Chem. Phys.* **103**, 2908 (1995); D. G. Evans, R. D. Coalson, H. J. Kim, and Y. Dakhnovskii, *Phys. Rev. Lett.* **75**, 3649 (1995).

<sup>13</sup>Y. Dakhnovskii and H. Metiu, *Phys. Rev. B* **51**, 4193 (1995).

<sup>14</sup>M. J. Hagmann, *Appl. Phys. Lett.* **66**, 789 (1995); M. J. Hagmann, *J. Vac. Sci. Technol. B* **14**, 838 (1996).

<sup>15</sup>A. Tikhonov, R. D. Coalson, and Y. Dahnovsky, *J. Chem. Phys.* (in press).

<sup>16</sup>See, for example, S. Mukamel, *Principles of Nonlinear Spectroscopy* (Oxford University Press, Oxford, 1995).

<sup>17</sup>Equation (12) and the formulas for electron current in Sec. II A were previously obtained in Refs. 8 and 9.

<sup>18</sup>Real metals are, of course, not perfect conductors; see, for example, F. Wooten, *Optical Properties of Solids* (Academic, New York, 1972). The effect of this departure from ideality remains to be investigated.

<sup>19</sup>V. M. Akulin, N. V. Karlov, *Intense Resonant Interactions in Quantum Electronics* (Springer-Verlag, Berlin, 1992).

<sup>20</sup>S.-I. Chu, in *Lasers, Molecules, and Methods*, edited by Joseph O. Hirschfelder, Robert E. Wyatt, and Rob D. Coalson (Vol. LXXIII in the Wiley Series on Advances in Chemical Physics, 1989).

<sup>21</sup>To see that  $a_{\alpha\beta}$  is actually dimensionless, it is useful to restore  $\hbar$ : " $\mathcal{E}_0(\mu_\alpha - \mu_\beta)/\hbar\omega$ ."

<sup>22</sup>A. Tikhonov, R. D. Coalson and Y. Dahnovsky (unpublished).

<sup>23</sup>Although the main purpose of these model calculations is to illustrate basic principles of laser-field driven electron transport through molecular wires, we should bear in mind the relevant frequency regime in real systems, which is given approximately by the energy difference between the Fermi level of the electrode and the highest occupied or lowest unoccupied molecular orbital of the bridge molecule, i.e., typically on the order of electron volts (Ref. 15).

<sup>24</sup>Note that in order to keep the  $a$  parameters fixed while varying the frequency, we must increase the laser field strength  $\mathcal{E}_0$  proportionally to  $\omega$  so that the ratio  $\mathcal{E}_0/\omega$  remains constant.